

CMOS front-end for the MDT sub-detector in the ATLAS Muon Spectrometer - development and performance

C. Posch¹, S. Ahlen¹, E. Hazen¹, J. Oliver²

¹ Boston University, Physics Department, Boston, USA

² Harvard University, Department of Physics, Cambridge, USA

Abstract

Development and performance of the final 8-channel front-end for the MDT segment of the ATLAS Muon Spectrometer is presented. This last iteration of the readout ASIC contains all the required functionality and meets the design specifications. In addition to the basic "amplifier-shaper-discriminator"-architecture, MDT-ASD employs a Wilkinson ADC within each channel for precision charge measurements on the leading fraction of the muon signal. The data will be used for discriminator time-walk correction, thus enhancing the spatial resolution of the tracker, and for chamber performance monitoring (gas gain, ageing etc.). It was also demonstrated that this data can be used for performing particle identification via dE/dX . A programmable pulse injection system which allows for automated detector calibration runs was implemented on the chip. Results of performance and functionality tests on prototype ASICs, both in the lab and on-chamber, are presented.

I. INTRODUCTION

The ATLAS muon spectrometer is designed for stand-alone measurement capability, aiming for a P_T resolution of 10% for 1 TeV muons. This target corresponds to a single tube position resolution of $< 80 \mu\text{m}$ which translates into a signal timing measurement resolution of $< 1 \text{ ns}$. The maximum hit rate is estimated 400 kHz per tube.

The ATLAS Monitored Drift Tube (MDT) system is composed of about 1200 chambers with each chamber consisting of several layers of single tubes. In total, there are about 370'000 drift tubes of 3 cm diameter, with lengths varying from 1.5 to 6 m.

The active components of the MDT on-chamber readout electronics are the MDT-ASD chip, which receives and processes the induced anode wire current signal, the AMT time-to-digital converter (TDC), which measures the timing of the ASD discriminator pulse edges, and a data concentrator/multiplexer/optical-fiber-driver (CSM) which merges up to 18 TDC links into one fast optical link and transmits the data to the off-detector readout driver (MROD).

II. CIRCUIT DESIGN

The MDT-ASD is an octal CMOS Amplifier-Shaper-Discriminator which has been designed specifically for the ATLAS MDT chambers [5]. System aspects and performance considerations force an implementation as an ASIC. A standard commercial $0.5\mu\text{m}$ CMOS process is used for fabrication.

The analog signal chain part of the MDT-ASD has been

described and presented previously [3] and will therefore be addressed only superficially in this article.

The MDT-ASD signal path is a fully differential structure from input to output for maximum stability and noise immunity. Each MDT connects to an "active" pre-amplifier with an associate "dummy" pre-amp. The input impedance of the pre-amps is 120Ω , the ENC of the order of $6000 e^- \text{ RMS}$, with a contribution of $4000 e^-$ from the tube termination resistor [2].

Following the pseudo-differential pair of pre-amps is a differential amplifier which provides gain and outputs a fully differential signal to two subsequent amplifier stages. These amplifiers supply further gain and implement the pulse shaping. In order to avoid active baseline restoration circuitry and tuneable pole/zero ratios, a bipolar shaping function was chosen [8][6].

The shaper has a peaking time of 15 ns and area balance of $< 500 \text{ ns}$. The sensitivity at the shaper output is specified $3 \text{ mV/primary } e^-$, or 12 mV/fC , with a linear range of 1.5 V or 500 primary e^- . The nominal discriminator threshold is 60 mV, corresponding to 20 primary e^- or $6 \sigma_{\text{noise}}$.

The bipolar shaping function in conjunction with the tube gas Ar/CO_2 93/7 with its maximum drift time of 800 ns and significant "R-t" non-linearity can cause multiple discriminator threshold crossings from a single traversing particle. The MDT-ASD uses an "artificial deadtime"-scheme to suppress these spurious hits.

In addition to the basic amplifier-shaper-discriminator-architecture, the MDT-ASD features one Wilkinson charge-to-time converter per channel, programmability of certain functional and analog parameters along with a JTAG interface, and an integrated pulse injection system.

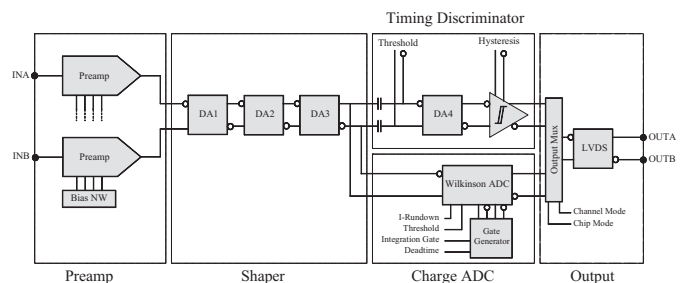


Figure 1. MDT-ASD channel block diagram

The shaper output is fed into the discriminator for leading edge timing measurement and into the Wilkinson ADC section for performing a gated charge measurement on the leading fraction of the tube signal (Figure 1). The information contained in the MDT-ASD output pulses, namely the leading edge timing and the pulse width encoded signal charge, are read and converted to digital data by a TDC [1].

A. Wilkinson ADC

The Wilkinson dual-slope charge-to-time converter operates by creating a time window of programmable width at the threshold crossing of the tube signal, integrating the signal charge onto a holding capacitor during that gate time, and then discharging the capacitor with a constant current. The rundown current is variable in order to adjust to the dynamic range of the subsequent TDC.

The Wilkinson cell operates under the control of a gate-generator which consists of all-differential logic cells. It is thus highly immune to substrate coupling and can operate in real time without corrupting the analog signals.

The main purpose of the Wilkinson ADC is to provide data which can be used for the correction of time-slew effects due to signal amplitude variations. Time slewing correction eventually improves the spatial resolution of the tracking detector and is necessary to achieve the specified 80 μ m single tube resolution. In addition, this type of charge measurement provides a useful tool for chamber performance diagnostics and monitoring (gas gain, tube ageing etc). Measurements of the Wilkinson conversion characteristics as well as the noise performance and non-systematic charge measurement errors of the Wilkinson ADC are shown in sections III.C and III.D.

The feasibility of the MDT system to perform particle identification via dE/dX measurement using the Wilkinson ADC was evaluated. The results of a simulation study on energy separation capability of the MDT system are published in [4].

B. Programmable parameters

It was found crucial to be able to control certain analog and functional parameters of the MDT-ASD, both at power-up/reset and during run time. A serial I/O data interface using a JTAG type protocol plus a number of associated DACs were implemented on the chip.

1) Timing discriminator

The threshold of the main timing discriminator is controllable over a wide range (up to > 4 times nominal) with 8-bit resolution. The discriminator also has adjustable hysteresis from 0 to 1/3 of the nominal threshold.

2) Wilkinson converter control

The *integration gate width* can be set from 8 ns to 45 ns in steps of 2.5 ns (4-bit). This setting controls what fraction of the leading part of the signal is used for conversion. The nominal gate width is 15 ns which corresponds to the average peaking time t_p of the pre-amplifier. It can be demonstrated that the time slewing is only correlated to the leading edge charge and not to the total signal charge of the MDT signal. ADC measurements with a gate > 2 \times t_p thus can not be used to further improve the spatial resolution of the system [6][7]. However for dE/dX measurements for particle identification, longer gates are desirable [4]. The current controlling the gate width is set by a binary-weighted switched resistor string.

The *discharge (rundown) current* of the integration capacitors is controlled by a 3-bit current DAC. This feature allows the ADC output pulse width to be adjusted to the dynamic range of the TDC (e.g. 200 ns @ a resolution of 0.78125 ns for AMT-1 [1]).

The end of one Wilkinson conversion cycle is triggered by a *second variable-threshold discriminator*. The setting of this threshold also affects the width of the Wilkinson output pulse but in principle does not influence the ADC performance significantly and is primarily implemented for troubleshooting and fine-tuning purposes.

3) Functional parameters

The *deadtime* setting defines an additional time window after each hit during which the logic does not accept and process new input. It can be set from 300 to 800 ns in steps of 70 ns (3 bit). The nominal setting is 800 ns corresponding to the maximum drift time in the MDT. This feature is used to suppress spurious hits due to multiple threshold crossings in the MDT signal tail and thus reducing the required readout bandwidth.

A number of set-up bits are designated to control *global settings* for single channels and the whole chip. For diagnostic (boundary scan interconnect testing etc.) and troubleshooting purposes, the output of each channel can be tied logic HI or LO. The chip itself can be set to work either in ToT (Time-over-threshold) or ADC mode (the output pulse contains the pulse-width encoded charge measurement information).

Table 1 summarizes the programmable parameters.

Table 1. MDT-ASD programmable parameters

PARAMETER	NOMINAL	RANGE	LSB	UNIT
DISC1 Threshold	60	-256 \div 256	2	mV
DISC1 Hysteresis	10	0 \div 20	1.33	mV
Wilkinson integration gate	14.5	8 \div 45	2.5	ns
DISC2 Threshold	32	32 \div 256	32	mV
Wilkinson discharge current	4.5	2.4 \div 7.3	0.7	μ A
Dead-time	800	300 \div 800	70	ns
Calibration channel mask	–	–	–	–
Calibration capacitor select	–	50 \div 400	50	fF
Channel mode	ON	ON, HI, LO	–	–
Chip mode	ADC	ADC, ToT	–	–

C. Calibration pulse injection

In order to facilitate chip testing during the design phase as well as to perform system calibration and test runs with the final detector assembly, a differential calibration/test pulse injection system was implemented on the chip. It consists of two parallel banks of 8 switchable 50 fF capacitors per channel and an associated channel mask register. The mask register allows for each channel to be selected separately whether or not it will receive test pulses. The capacitors are charged with external voltage pulses, nominal 200 mV swing standard LVDS pulses, yielding an input signal charge range of 10 – 80 fC. The pulse injection system enables fully automated timing and charge conversion calibration of the MDT sub-detector. Calibration runs are required for example after changes in certain setup parameters.

III. TEST RESULTS

The MDT-ASD has been prototyped extensively. The last iteration, ASD01A, is a fully functional 8-channel prototype and is considered to be the final production design. Results of functionality and performance tests on this prototype, indicate that the ATLAS MDT front-end is ready for mass-production¹.

A. Pre-amp - Shaper: Sensitivity

Figure 2 shows oscilloscope traces of the shaper output at the threshold coupling point. The measurements were taken with a calibrated probe using well defined input charges. The peaking time of the delta pulse response (time between the arrows) is 14.4 ns. There is a probe attenuation of 10:1 which is not accounted for in the peak voltage values in the left hand column. Due to the differential architecture, the voltages have to be multiplied by a factor 2 to obtain the total gain (Figure 3).

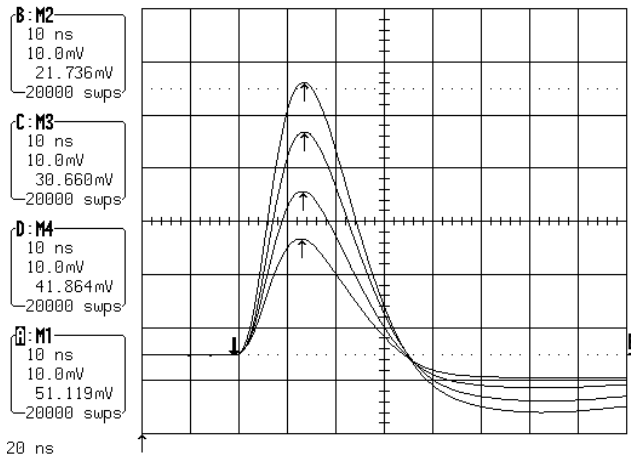


Figure 2. Shaper output for 40, 60, 80 and 100 fC input charge. The peak voltages translate into the sensitivity curve below by multiplying with a factor of two (single-ended to differential) and taking into account a probe attenuation of 10:1.

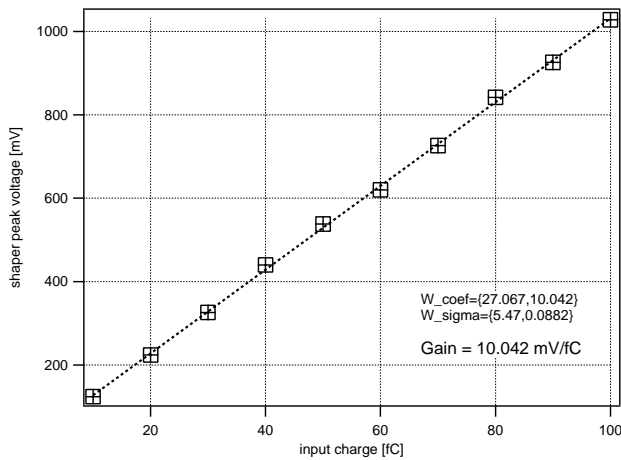


Figure 3. Sensitivity of the analog signal chain (Pre-amp to shaper) for the expected input signal range. The gain amounts to 10 mV/fC, exhibiting good linearity.

¹ Aspects of radiation tolerance have not been addressed in this article, however results of radiation tests on the process and the prototype chips indicate that ATLAS requirements are met.

B. Discriminator time slew

Due to the finite rise time of the signal at the discriminator input, different signal amplitudes with respect to the threshold level produce different threshold crossing times. This effect is called time slew. Figure 4 shows the time slew as measured for a constant threshold by varying the input charge. The time slew over the expected muon charge range ($\sim 20 - 80$ fC) is of the order 2 ns. Comparing this number to the requirements, it becomes obvious that slew correction through charge measurement is an essential feature of the MDT-ASD.

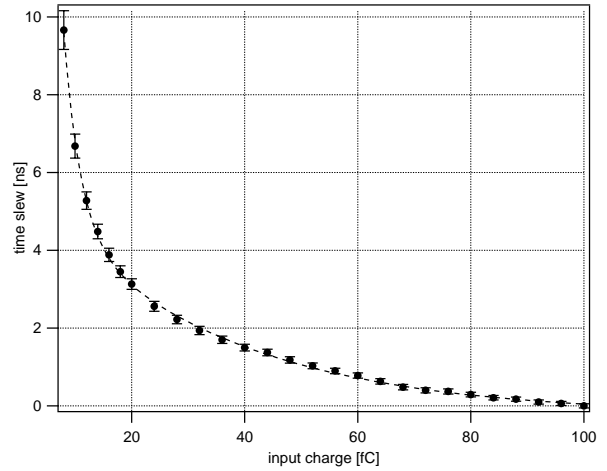


Figure 4. Time slew of the MDT-ASD signal chain. The data display the timing of the discriminator 50% point of transition as a function of input signal amplitude for a 20 mV threshold.

C. Wilkinson ADC performance

The transfer characteristic of the Wilkinson charge ADC is plotted in Figure 5. The traces show the non-linear relation between input charge and output pulse width for 4 different integration gates. The advantage of this compressive characteristic is that small signals which require a higher degree of time slew correction gain from a better charge measurement resolution. The disadvantage is an increased number of calibration constants. The dynamic range spans from 90 ns (8 ns gate) to 150 ns (45 ns gate).

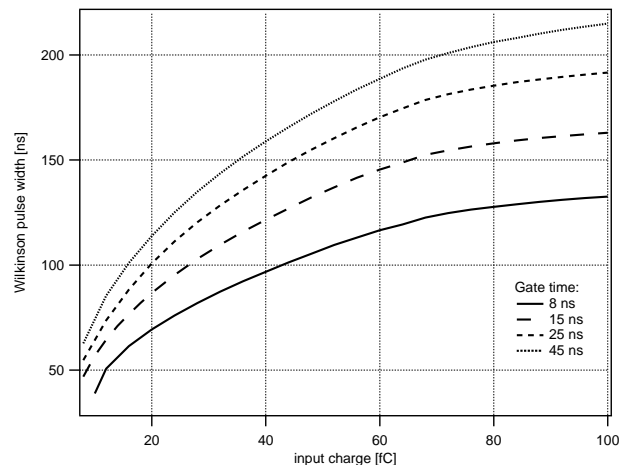


Figure 5. Wilkinson ADC output pulse width as a function of input charge for 4 different integration gate widths

D. Noise performance and non-systematic measurement errors

The timing information carried by the ASD output signal is recorded and converted by the AMT (Atlas Muon TDC) time-to-digital converter. The AMT can be set to provide a dynamic range for the pulse width measurement of 0 - 200 ns with a bin size of 0.78 ns [1]. If the ASD is programmed to produce output pulses up to a maximum of 200 ns, then the combination of the ASD and the AMT chip represents a charge-ADC with a resolution of 7 - 8 bits.

Non-systematic errors in the timing and charge measurement due to electronic noise in the ASDs and AMTs and quantization errors set a limit to the performance of the system. The following two sections present test results on the noise performance of the MDT-ASD and determine how the noise introduces error and degrades the accuracy of the measurements.

1) Time measurement

Figure 6 shows the measured RMS error of the leading edge time measurement at the output of the ASD as a function of signal charge. The lower curve gives the noise for floating pre-amplifier inputs while the upper curve includes the effect of the 380 Ω tube termination resistor. The threshold is set to its nominal value of 60 mV (corresponding to ~ 5 fC). The horizontal axis gives the charge of the input signal applied through the test pulse injection system. Typical muon signals are expected to be in the range of 20 - 80 fC, resulting in a RMS error of the order of 200 ps.

The time-to-digital conversion in the AMT shows a RMS error of 305 ps, including 225 ps of quantization error [1]. The resulting total error of the time measurement, covering all internal noise sources from the front-end back to the A/D conversion, will typically be of the order of 360 ps RMS.

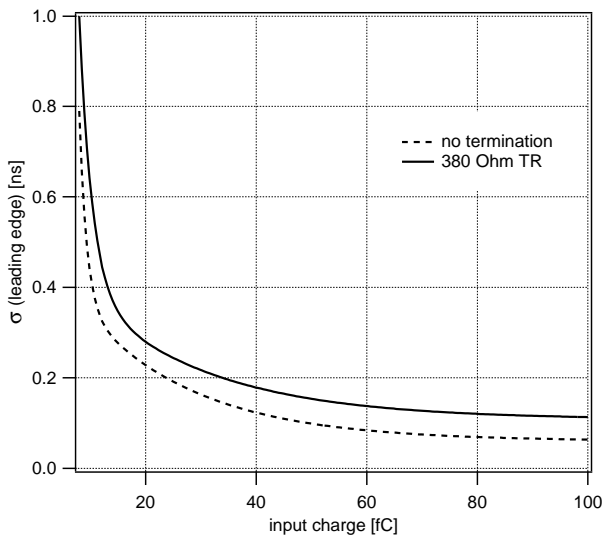


Figure 6. RMS error of the leading edge timing measurement vs. input charge for a fixed discriminator threshold (set to its nominal value of 60 mV or 5 fC). Typical muon signals will be of the order of 40 - 50 fC. Bottom curve: floating pre-amp input, top curve: with 380 Ω tube termination resistor.

2) Charge measurement

Measurement errors in the pulse width at the ASD output are typically below 600 ps RMS, depending on signal amplitude and integration gate width. Figure 7 shows the ASD Wilkinson noise versus signal amplitude in percent of the measured charge for 3 short integration gate widths. The pulse width conversion (two independent pulse-edge conversions) in the AMT exhibits a RMS error of 430 ps including quantization error. Hence, the resulting total error, covering all internal noise sources from the front-end back to the A/D conversion, stays in the range of under 800 ps RMS. This number corresponds to a typical error of well below 1% of the measured charge for the vast majority of signals.

The effect of the tube termination resistor can be seen in Figure 8. Contributing about 4000 e⁻ ENC, this termination resistor constitutes the dominant noise source of the read-out system.

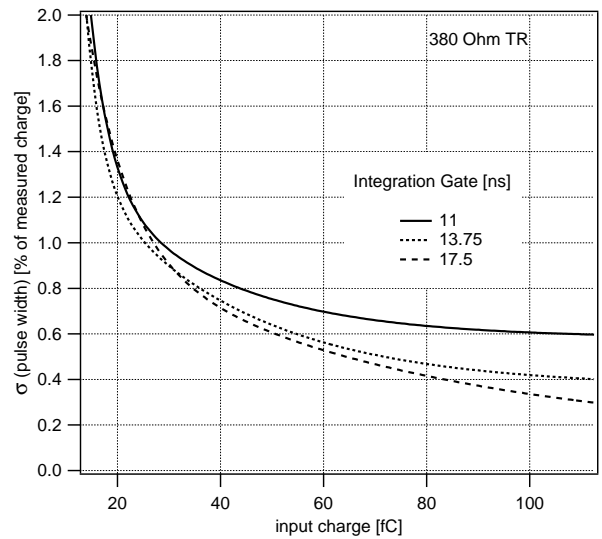


Figure 7. RMS error of Wilkinson pulse width at the output of the ASD as a function of input signal charge for a fixed discriminator threshold (nominal), given in percent of the measured charge. Note the decrease in noise for growing integration gate widths.

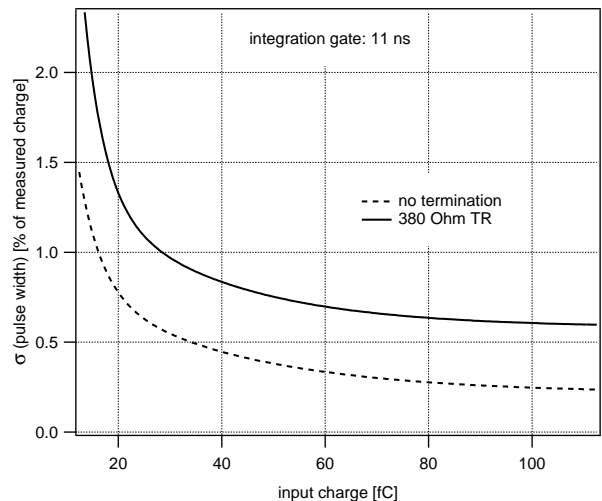


Figure 8. Effect of the 380 Ω tube termination resistor on the charge measurement error.

All systematic charge measurement errors e.g. due to converter non-linearities or channel-to-channel variations can be calibrated out using the ASD's programmable test-pulse injection system.

IV. ON-CHAMBER TESTS WITH A COSMIC RAY TEST SETUP

A cosmic ray test stand has been set up at Harvard University. The system with one Module-0 endcap chamber (EIL type) and a trigger assembly of 4 scintillator stations records > 1 GeV cosmic muons. The read-out electronics employs an earlier 4-channel prototype of the ASD, mounted on "mezzanine" boards, each of which services 24 tubes. This earlier ASD version does not contain a Wilkinson ADC or a test-pulse circuit, but for the purposes of this test it is functionally equivalent to the latest prototype. An extensive description of this test stand and presentation of the analysis methods and results are the subject of a forthcoming ATLAS note by S. Ahlen.

A histogram of TDC values for single-muon 8-tube events is shown in Figure 9. The maximum drift time is seen to be about 1000 channels (780 ns).

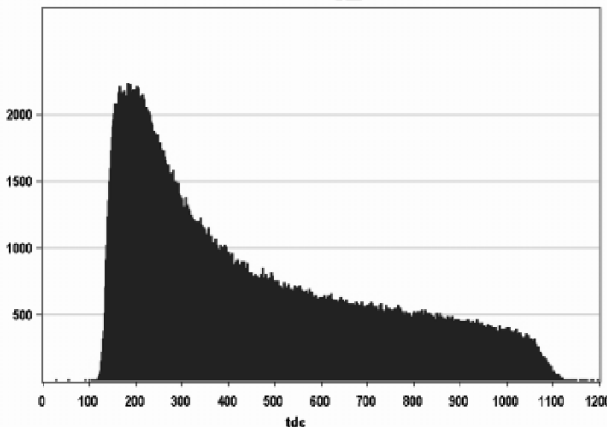


Figure 9. TDC spectrum produced on the cosmic ray test stand.

A track fitting program to evaluate chamber resolution has been developed. The procedure first obtains fits using the four tubes of each multilayer. These fits determine the most likely position of the global trajectory relative to the drift tube wire by considering all 16 possibilities for each multilayer. Then a global 8-tube straight-line-fit is done using this information, and then the two most poorly fit tubes are rejected and a final 6-tube fit is accomplished. This last step rejects delta rays, poor fits for near-wire hits, and large multiple scatters. With no additional data cuts a single tube tracking resolution of about $100 \mu\text{m}$ (and nearly 100% efficiency) is obtained.

By requiring consistency of the slopes of the 4-tube fits in the two multilayers (4 mrad) more multiple scatters and delta rays are rejected. The result of this cut is that the single tube spatial resolution improves to about $70 \mu\text{m}$ with about 45% efficiency.

Figure 10. shows the distribution of the residuals representing the distances from the fitted track line to the time circles around the wires.

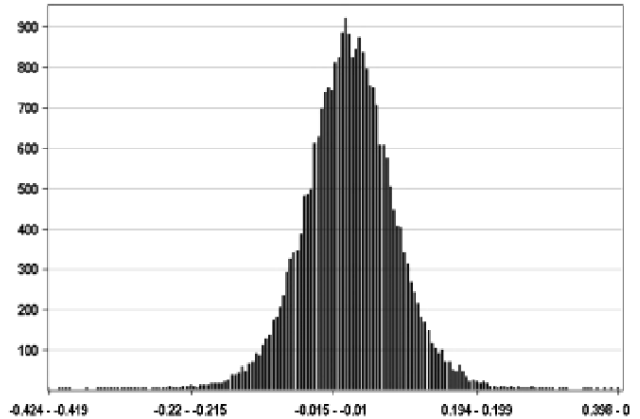


Figure 10. Spatial resolution of the EIL chamber on the cosmic ray test stand (horizontal axis in mm)

More detailed studies of the MDT resolution are underway at several sites, but these initial results suggest that the ASD-based front-end electronics can provide the required precision under operational conditions.

V. CONCLUSIONS

Development, design and performance of the 8-channel CMOS front-end for the MDT segment of the ATLAS Muon Spectrometer has been presented. The device is implemented as an ASIC and fabricated using a standard commercial $0.5 \mu\text{m}$ CMOS process. Irradiation data on the fabrication process and on the prototype chip exist and indicate that ATLAS radiation hardness standards are met.

Results of functionality and performance tests, both in the lab and on-chamber demonstrate that the ATLAS MDT front-end is ready for mass-production.

VI. REFERENCES

- [1] Y.Arai, Development of front-end electronics and TDC LSI for the ATLAS MDT, NIM in Physics Research A 453 (2000) 365-371, 2000.
- [2] J. Huth, A. Liu, J. Oliver, Note on Noise Contribution of the Termination Resistor in the MDTs, ATLAS Internal Note, ATLAS-MUON-96-127, CERN, Aug. 1996.
- [3] J. Huth, J. Oliver, W. Riegler, E. Hazen, C. Posch, J. Shank, Development of an Octal CMOS ASD for the ATLAS Muon Detector, Proceedings of the Fifth Workshop on Electronics for LHC Experiments, CERN/LHCC/99-33, Oct. 1999.
- [4] G. Novak, C. Posch, W. Riegler, Particle identification in the ATLAS Muon Spectrometer, ATLAS Internal Note, ATLAS-COM-MUON-2001-020, CERN, June 2001.
- [5] C. Posch, E. Hazen, J. Oliver, MDT-ASD, CMOS front-end for ATLAS MDT, ATLAS Internal Note, ATLAS-COM-MUON-2001-019, CERN, June 2001.
- [6] W. Riegler, MDT Resolution Simulation - Front-end Electronics Requirements, ATLAS Internal Note, MUON-NO-137, CERN, Jan. 1997.
- [7] W. Riegler, Limits to Drift Chamber Resolution, PhD Thesis, Vienna University of Technology, Vienna, Austria, Nov. 1997.
- [8] W. Riegler, M. Aleksa, Bipolar versus unipolar shaping of MDT signals, ATLAS Internal Note, ATLAS-MUON-99-003, March 1999.